DALTON
FULL PAPER

Crystal supramolecular motifs for $[Ph_4P]^+$ salts of $[M(mnt)_2]^{2-}$, $[M(mnt)_2]^-$, $[\{M(mnt)_2\}_2]^{2-}$, $[M(mnt)_3]^{3-}$ and $[M(mnt)_3]^{2-}$ (mnt^{2-} = maleonitriledithiolate)†

Gareth R. Lewis* and Ian Dance

School of Chemistry, University of New South Wales, Sydney 2052, Australia.
E-mail: I.Dance@unsw.edu.au

Received 6th January 2000, Accepted 18th July 2000
Published on the Web 29th August 2000

The crystal structures of $[Ph_4P]_2[M(mnt)_2]$ (M = Zn **1**, Cu **2** or Ni **3**), $[Ph_4P][M(mnt)_2]$ (M = Cu **4** or Ni **5**), $[Ph_4P]_2[\{M(mnt)_2\}_2]$ (M = Co **6** or Fe **7**), $[Ph_4P]_2[M(mnt)_3]$ (M = Fe **8** or Cr **10**) and $[Ph_4P]_3[Cr(mnt)_3]$ **9** {mnt = maleonitriledithiolate, $[S_2C_2(CN)_2]^{2-}$} have been determined to investigate the packing and supramolecular motifs in crystals containing $[Ph_4P]^+$ cations and $[M(mnt)_n]^{z-}$ anions. Seven different crystal packings are described. Crystals **2** are isomorphous with **3**, as are **4** with **5**, and **6** with **7**, and two dimorphs of **8** were identified (orthorhombic α-**8** and monoclinic β-**8**). The lattices of all compounds with planar (**2**, **3**, **4**, **5**) or approximately planar (**6**, **7**) anions contain segregated parallel stacks of anions (canted to the stack axis) and columns of embracing $[Ph_4P]^+$ cations. The structures of **2** and **3** contain approximately linear sequences of alternating sixfold phenyl embraces (6PE) and offset-face-to-face (OFF) motifs between cations, while the structures of **4**, **5**, **6** and **7** contain linear chains of cations engaged in translational fourfold phenyl embraces (4PE). Where the anions are not planar (tetrahedral **1** or octahedral **8**–**10**), OFF interactions between planar subsections of the anions (*i.e.* mnt ligands) and planar subsections of the cations (*i.e.* phenyl rings) occur, as a concerted motif involving four ions (**1**), or as a new sandwich motif (α-**8**, β-**8**). This sandwich motif, Ph · · · mnt · · · Ph, occurs for one mnt ligand per anion in α-**8**, and two mnt ligands per anion in β-**8**. Calculated energies are reported. Weak C–H · · · S and C–H · · · N hydrogen bonds occur in all structures, and appear to control the details of the commensurability between chains of cations and stacks of anions. Edge-to-face (EF) motifs between phenyl rings and mnt ligands do not occur. All crystals except one (**9**) are devoid of solvent, implying an absence of shape awkwardness in crystals of this type. The crystal packing of the related compound $[MePh_3P][Ni(mnt)_2]$ contains columns of stacked parallel fourfold phenyl embracing cations, parallel to stacked anions.

Introduction

In previous papers we have described the supramolecular motifs formed by the Ph_4P^+ cation in crystals. In these, the primary motifs are edge-to-face (EF) and offset-face-to-face (OFF) interactions between phenyl rings.[1,2] These operate in concert forming secondary motifs, of which the main types are the sixfold phenyl embrace (6PE) and several fourfold phenyl embraces (4PE).[2] The 6PE comprises six EF primary motifs, the orthogonal 4PE comprises four EF motifs, and the parallel 4PE comprises two EF and one OFF motif. These secondary motifs associate further to form tertiary motifs, such as zig-zag infinite chains of 6PE (ZZI6PE),[3] the linear infinite chain of translational 4PE (LIT4PE),[3] and, for cations Ph_3RP^+, the hexagonal array of 6PE (HA6PE).[4,5] In some crystals these associate further into quaternary supramolecular motifs which extend throughout the crystal lattice.[6,7] The net *attractive* energy for a 6PE between two Ph_4P^+ cations is in the range 8–11 kcal mol^{-1}, which is comparable with the intermolecular energy of the stronger hydrogen bonds.[8]

Clearly the size, shape and charge of the anion associated with Ph_4P^+ will influence the crystal packing. Our previous analyses have demonstrated that the secondary motifs formed by Ph_4P^+ can be associated with a considerable variety of anions, large and small, and that there are some relationships between the type of tertiary motif and the charge/dimension of the anion, because chains of cations and stacks of anions must be commensurate in crystals.[3,9]

In this context, the class of homoleptic metal dithiolene complexes[10–13] provides a valuable set of anions. In this paper we report on complexes of the mnt (maleonitriledithiolate) ligand, with R = CN.

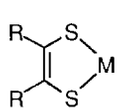

These electronically non-innocent complexes are electron transfer active, with a variable redox level (delocalised over metal and ligand), which provides anions with the same shape but different charge. These metal complex anions can therefore be deployed to vary cation–anion stoichiometry, without variation of the anion size or shape. Metal variation allows different stereochemistry for the same charge. Molecular stereochemistries for the dithiolene complex anions are tetrahedral $[M(mnt)_2]^{2-}$, square planar $[M(mnt)_2]^z$, five-coordinate dimeric $[\{M(mnt)_2\}_2]^{2-}$, and octahedral $[M(mnt)_3]^z$: trigonal prismatic stereochemistry also occurs for some relatively oxidised tris-(dithiolene) complexes. We report here on crystalline $[Ph_4P]_2[M(mnt)_2]$ (M = Zn **1**, Cu **2** or Ni **3**), $[Ph_4P][M(mnt)_2]$ (M = Cu **4** or Ni **5**), $[Ph_4P]_2[\{M(mnt)_2\}_2]$ (M = Co **6** or Fe **7**), $[Ph_4P]_2$-

† Electronic supplementary information (ESI) available: crystallisation details and selected interatomic distances for salts **1**–**10**; parameters used to define the coordination geometry in **8**–**10**; figures showing 4PE and OFF motifs, hydrogen bonding and layered structures for some of the salts. See http://www.rsc.org/suppdata/dt/b0/b000093k/

 DOI: 10.1039/b000093k

$[M(mnt)_3]$ (M = Fe **8** or Cr **10**) and $[Ph_4P]_3[Cr(mnt)_3]$ **9**. Amongst this set there are comparisons of (a) planar and tetrahedral $[M(mnt)_2]^{2-}$, (b) planar $[M(mnt)_2]^{2-}$ and planar $[M(mnt)_2]^{-}$, (c) planar $[M(mnt)_2]^{-}$ and dimeric $[\{M(mnt)_2\}_2]^{2-}$, and (d) octahedral $[M(mnt)_3]^{2-}$ and octahedral $[M(mnt)_3]^{3-}$. These anions thus allow systematic investigation of separated variables in the crystal packing with $[Ph_4P]^+$ cations.

One aspect of crystalline metal dithiolene complexes that has already been investigated is the stacking of planar complexes. Structural studies on four-coordinate metal dithiolenes have shown that the compounds may appear as isolated units, dimers with M–S bonds, M–M bonded dimers, or partially oxidised one-dimensional stacks with M–M bonds and varying degrees of pairing distortion.[14] Charge-transfer complexes incorporating $[M(mnt)_2]^-$ (M = Ni, Pd or Pt) anions have been shown to display pressure-dependent conductivity,[15] unusual electronic[16] and magnetic properties,[17] and ferromagnetism.[18] In each case the bulk properties are due to the stacks of anions formed in the solid state. Mixed stacks with planar cations are also well-known.[19,20]

Homoleptic mnt complexes have a spikey periphery, caused by the rigid protuberances of the cyanide groups from a relatively small coordination core. This has consequences for crystal packing. Therefore, we have investigated crystals of compounds **1** to **10**. We have examined the crystal packing and supramolecular motifs, considered the competition between the known cation · · · cation motifs and anion · · · anion association motifs, and explored for new cation · · · anion motifs. While most of the previous work with metal–mnt anions has used alkylammonium cations, or planar organic cations, there are in the Cambridge Structural Database some relevant crystal structures, namely $[AsPh_4]_2[M(mnt)_2]$ (M = Ni,[21] Cu,[22] Zn[22] or Te[23]), $[AsPh_4]_2[M(mnt)_3]$ (M = Fe,[24] Mo,[25] Tc[26] or W[25]), and $[MePh_3P][Ni(mnt)_2]$,[27] and these are included in our analyses.

The objective of this research is to recognise and understand the crystal supramolecular motifs for molecular ions, here specifically $[Ph_4P]^+$ and $[M(mnt)_n]^{z-}$ ions, such that they can then be deployed in crystal design and engineering.

Results

Synthesis and methodology

The salts were prepared generally by the reaction of metal halides with $Na_2(mnt)$ in water or EtOH, followed by metathesis with Ph_4PBr. The initial precipitates were purified from hot acetone/^{t}BuOH to give pure products in good yield. Single crystals for X-ray diffraction studies were grown by the slow diffusion of a concentrated solution of the salt in a polar solvent into a less polar solvent (see Supplementary Information, Table S1).

X-Ray powder diffraction measurements of a bulk sample of $[Ph_4P][Ni(mnt)_2]$ **5** showed the occurrence of the pure phase of the structure described. Analogous measurements of $[Ph_4P][Cu(mnt)_2]$ **4** indicated that the structure is isomorphous with **5**. Similar measurements showed the salt $[Ph_4P]_2[\{Fe(mnt)_2\}_2]$ **7** to be isomorphous with the structure of $[Ph_4P]_2[\{Co(mnt)_2\}_2]$ **6** detailed below.

Two crystal forms of $[Ph_4P]_2[Fe(mnt)_3]$ **8** were obtained from the same crystallisation of the pure salt, by slow infusion of an acetone solution into diethyl ether. The crystals with a cubic habit, denoted α-**8**, have orthorhombic crystal symmetry, whilst those which are diamondoid have a monoclinic lattice, β-**8**. It is thought that the monoclinic dimorph, β-**8**, is the kinetic form as these crystals were isolated from the crystallisation after a shorter period of time (2 days) than the orthorhombic dimorph, α-**8** (6 days, Table S1). The hypothesis that α-**8** is the thermodynamically stable form is supported by the isomorphism of α-**8** with the previously reported structures $[AsPh_4]_2[M(mnt)_3]$ (M = Fe,[24] Mo,[25] Tc[26] or W[25]), all of which are orthorhombic.

Table 1 Parameters used in the calculations of interatomic energies. See text for definition of symbols

Atom type	r^a_i/Å	e^a_i/kcal mol^{-1}	Atom partial charges	
Cation				
P	2.10	0.200	+0.40	
C	1.95	0.093	−0.10	
H	1.60	0.020	+0.15	
Anions				
			Anion of **1**	Anion of **8**[a]
N	2.05	0.065	−0.35	−0.40
C≡N	2.05	0.150	+0.15	+0.15
C=C	1.95	0.080	+0.10	+0.10
S	2.10	0.200	−0.40	−0.35
Zn	2.20	0.150	+0.20	
Fe	2.20	0.130		+0.70

[a] Same partial charge values used for both crystal forms.

Intermolecular energies E were calculated as the sum of the interatomic energies,[28,29] using the Lennard–Jones 6–12 interatomic potential for van der Waals energies E^{vdw}_{ij}, and the coulombic components $E^{coulombic}_{ij}$, as described previously.[6,7,30,31] The atom partial charges q_i were obtained from a QEq calculation[32] using the CERIUS^2 software.[33] The computed partial charges sum to +1 for each $[Ph_4P]^+$ cation, and to $-z$ for each $[M(mnt)_n]^{z-}$ anion. The parameters and charges are presented in Table 1: d_{ij} is the interatomic separation; e^a_{ij} ($=\{e^a_i\, e^a_j\}^{0.5}$) and d^a_{ij} ($=r^a_i + r^a_j$) are respectively the energy depth and the interatomic distance for the attractive well of the vdW potential;[30] and the permittivity ε was set equal to d_{ij}.[30] Volumes were computed using a Connolly surface[34,35] with a probe sphere of radius 1.4 Å, using the CERIUS^2 software.[33]

Crystal and refinement details are given in Table 2: **2** and **3** are isomorphous, as are **4** and **5**, and **6** and **7**. Details of the molecular structures of **1**–**10** are provided as Supplementary Information, Table S2.

Molecular structures

The molecular structures and metrical properties of the anions and cations are normal. In **1**, $[Zn(mnt)_2]^{2-}$ is tetrahedral, whilst the nickel and copper complexes of $[M(mnt)_2]^{2-}$ **2** (Cu) isostructural with **3** (Ni) and $[M(mnt)_2]^{-}$ **4** (Cu) isostructural with **5** (Ni) are square planar with the metal atoms located on crystallographic inversion centres. The metal atoms of $[\{Co(mnt)_2\}_2]^{2-}$ **6** and isostructural $[\{Fe(mnt)_2\}_2]^{2-}$ **7** have square pyramidal geometry, with the metal atom coordinated to four sulfur atoms in the basal plane and one sulfur atom of the neighbouring $M(mnt)_2$ moiety bound at the axial site. The iron and chromium tris(mnt) complexes $[Fe(mnt)_3]^{2-}$ **8**, $[Cr(mnt)_3]^{2-}$ **10**, and $[Cr(mnt)_3]^{3-}$ **9**, are octahedral (see Supplementary Information). The chromium salt **9** is the first $[M(mnt)_3]^{3-}$ complex to be structurally characterised. The bond distances within the mnt ligands are consistent with those found in comparable structures. The metal–sulfur bonds of **3** and **9** are longer than those in their corresponding oxidised species, **5** and **10** respectively (see Supplementary Information).

Crystal packing

Tetrahedral dianion: $[Zn(mnt)_2]^{2-}$. The crystal structure of $[Ph_4P]_2[Zn(mnt)_2]$ **1**, isostructural with $[AsPh_4]_2[Zn(mnt)_2]$,[22] contains a matrix of cations and anions, with no regular embraces between the cations, and well separated anions. The most significant features are between cations and anions. Since

Table 2 Crystal data for **1–10**

Salt	**1**	**2**	**3**	**5**	**6**	**α-8**	**β-8**	**9**·0.75Me_2CO	**10**
Empirical formula	$C_{54}H_{40}N_4P_2S_4Zn$	$C_{54}H_{40}N_4CuP_2S_4$	$C_{54}H_{40}N_4NiP_2S_4$	$C_{32}H_{20}N_4NiPS_4$	$C_{64}H_{40}N_8Co_2P_2S_8$	$C_{60}H_{40}FeN_6P_2S_6$	$C_{60}H_{40}FeN_6P_2S_6$	$C_{86.25}H_{64.5}CrN_6O_{0.75}P_3S_6$	$C_{60}H_{40}N_6CrP_2S_6$
M	1024.47	1022.64	1017.81	678.44	1357.32	1155.13	1155.13	1534.21	1151.28
Crystal system	Monoclinic	Monoclinic	Monoclinic	Monoclinic	Monoclinic	Orthorhombic	Monoclinic	Monoclinic	Orthorhombic
Space group (no.)	$P2_1/c$ (14)	$P2_1/n$ (14)	$P2_1/n$ (14)	$P2_1/c$ (14)	$P2_1/n$ (14)	*Pbcn* (60)	*C*2/*c* (15)	$P2_1/c$ (14)	*Pbcn* (60)
a/Å	17.5248(7)	11.148(2)	11.223(2)	8.242(2)	7.1391(14)	20.401(5)	27.978(6)	24.5937(9)	20.290(5)
b/Å	16.7568(7)	15.318(3)	15.164(3)	16.083(3)	16.085(4)	15.487(4)	13.402(3)	14.7251(6)	15.548(4)
c/Å	18.3862(7)	14.587(3)	14.670(3)	24.806(5)	26.993(7)	17.965(4)	19.882(4)	25.2038(10)	17.986(4)
α/°	90.000	90.000	90.000	90.000	90.000	90.000	90.000	90.000	90.000
β/°	110.155(10)	96.92(3)	95.90(3)	105.24(3)	90.83(3)	90.000	130.09(3)	117.822(10)	90.000
γ/°	90.000	90.000	90.000	90.000	90.000	90.000	90.000	90.000	90.000
V/Å^3	5068.7(4)	2472.7(9)	2483.6(8)	3172.6(11)	3099.3(11)	5676(2)	5703(2)	8072.3(5)	5674(2)
Z	4	2	2	4	2	4	4	4	4
μ/mm^{-1}	0.754	0.718	0.666	0.985	0.904	5.077	5.053	0.405	0.523
Reflections collected	32774	4347	4364	5584	15063	5378	5405	56320	38090
Independent reflections	12030	4364	4364	5584	4684	5378	5405	10555	3270
R_{int}	0.0684	0.0574	0.0622	0.0239	0.0722	0.0235	0.0381	0.0781	0.0431
Final R_1 [$I > 2\sigma(I)$], wR_2	0.0414, 0.0640	0.0383, 0.0830	0.0409, 0.1056	0.0337, 0.0875	0.0416, 0.0552	0.0330, 0.0720	0.0334, 0.1006	0.0438, 0.0939	0.0649, 0.1573

Fig. 1 The embrace between a pair of $[Ph_4P]^+$ ions (light tones) and a pair of $[Zn(mnt)_2]^{2-}$ ions (dark tones) in **1**. The four offset-face-to-face interactions in this centrosymmetric motif are L1 · · · R1, L2 · · · R2′, L1′ · · · R1′ and L2′ · · · R2.

Fig. 2 View along the *c*-axis of $[Ph_4P]_2[Cu(mnt)_2]$ **2** showing the parallel chains of cations and stacks of strongly canted anions. H atoms are omitted.

both the cation and anion have tetrahedral stereochemistry about the central atom, a tetrahedral-Ph_4P^+ · · · tetrahedral-$[Zn(mnt)_2]^{2-}$ embrace could have been expected, analogous to the orthogonal 4PE which occurs between Ph_4P^+ ions.[2] However, this is thwarted by a mismatch of the locations and extensions of the mnt and phenyl groups, as shown in Fig. S1 of the Supplementary Information. Instead, there is an effective embrace which involves a pair of cations and a pair of anions and is comprised of four OFF Ph · · · mnt interactions, as illustrated in Fig. 1.

There are also weak hydrogen bonds between the cations and anions, involving the phenyl rings orthogonal to the plane of the mnt ligand, to give near linear C–H · · · S and C–H · · · N weak hydrogen bonds (Fig. S2). The CH · · · N distances are typically *ca.* 2.85 Å and CH · · · S 2.90 Å.

Planar dianions: $[M(mnt)_2]^{2-}$. $[Ph_4P]_2[Cu(mnt)_2]$ **2**, $[Ph_4P]_2[Ni(mnt)_2]$ **3**, and $[AsPh_4]_2[Ni(mnt)_2]$ (CSD refcode KAKLUD)[15] are isomorphous, space-group $P2_1/n$. The lattice consists of parallel chains of cations and stacks of anions, shown in Fig. 2. The chain of Ph_4P^+ cations is comprised of 6PE motifs alternating with OFF interactions (involving a pair of phenyl groups in offset-face-to-face geometry): see Fig. 3 and Supplementary Information, Fig. S3. This secondary motif for Ph_4P^+ cations (6PE–OFF–6PE–OFF) occurs in other crystal structures.[36,37] The repeat distance for 6PE–OFF in **2** is 14.6 Å (=*c*). The $[Cu(mnt)_2]^{2-}$ anions are strongly canted to their stack axis, which allows the repeat length along this stack to match that of the cation chain: the N · · · N length of an anion is 10.6 Å. This provides a description but not a rationalisation of the crystal

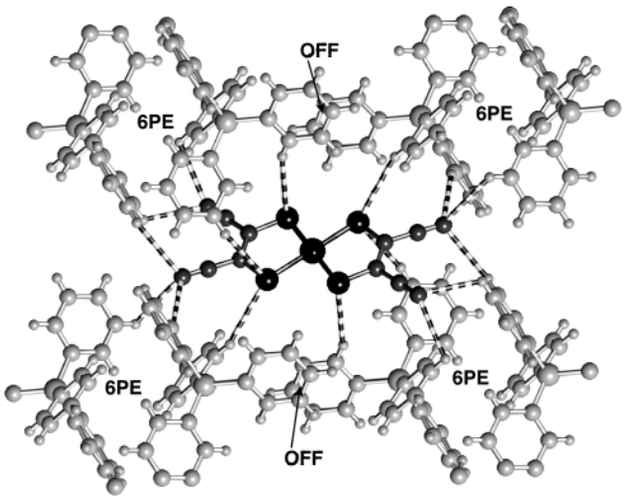

Fig. 3 Two chains of cations surrounding one $[Cu(mnt)_2]^{2-}$ anion in **2**, with the more effective C–H · · · S and C–H · · · N interactions marked as candystripes. Typical CH · · · N distances are 2.9 Å, CH · · · S distances 3.1 Å, and the C–H · · · S angles are >150°. C–H · · · N angles range down to 120°.

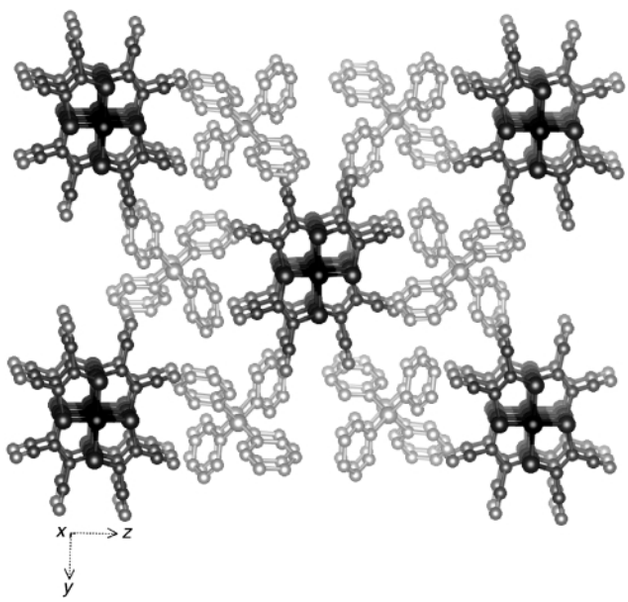

Fig. 4 Stacks of $[Ni(mnt)_2]^-$ anions (darker) and columns of cations (lighter) parallel to the *a*-axis in **5**. The planar anions are canted to and rotated about the stack axis, causing an expanded profile in this projection. Hydrogen atoms are omitted.

packing. Alternative arrangements can be envisaged. In particular, the ZZI6PE secondary motif for Ph_4P^+ cations, with the sequence 6PE–6PE–6PE–6PE has a shorter characteristic repeat length of *ca.* 11 Å,[3] and could allow a similar structure but with a lesser canting of the anions in their stacks. The non-occurrence of this established crystal packing type implies that there are additional factors in **2**, and these are the C–H · · · S and C–H · · · N weak hydrogen bonds from cations to anions. The shorter of these are shown in Fig. 3. On the basis of the dimensions it appears that the C–H · · · S interactions are more effective, but the C–H · · · N interactions are more numerous.

Planar monoanions: $[M(mnt)_2]^-$. Crystals of $[Ph_4P][Cu(mnt)_2]$ **4** and $[Ph_4P][Ni(mnt)_2]$ **5** are isomorphous, in space-group $P2_1/c$: the structure of **5** will be described. The anion is centrosymmetric. The crystal packing is again dominated by columns of cations and stacks of anions, which are shown in Fig. 4: there are six cation columns around each anion stack. The planar anions are not eclipsed in their stack, but displaced

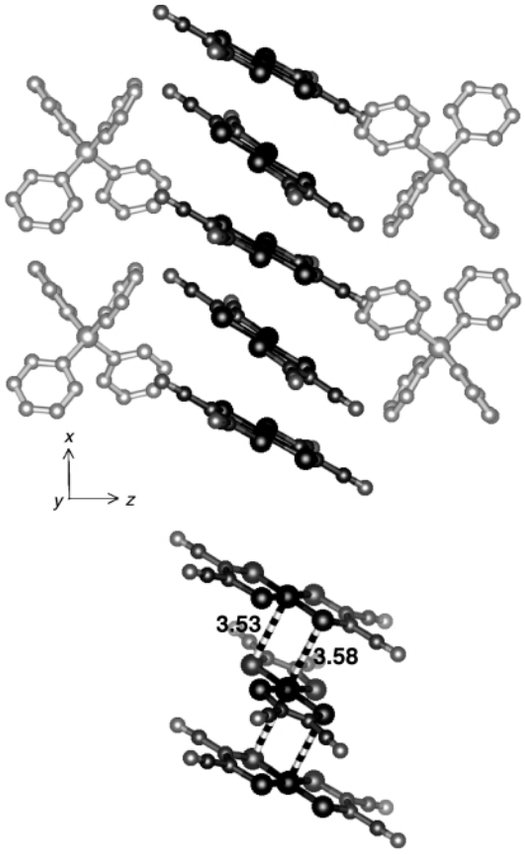

Fig. 5 The tilting of the $[Ni(mnt)_2]^-$ anions in **5** relative to their stack axis and the columns of Ph_4P^+ cations. The *a*-axis repetition is the P · · · P separation and the separation of alternate Ni atoms. The lower section shows detail of the relationship between adjacent centrosymmetric $[Ni(mnt)_2]^-$ anions in the anion stack of **5**.

and rotated, enlarging the projection cross-section of the anion stack. The cations form an established tertiary motif, the linear infinite chain of translational 4PE (LIT4PE),[3] in which the orthogonal fourfold phenyl embrace between adjacent cations is translated in a linear fashion along the column. Each Ph_4P^+ cation is engaged in two 4PE, and each 4PE has four concerted EF primary interactions. In **5** the repeat distance in the column, the P · · · P separation of the 4PE, is the unit cell *a*-axis length of 8.24 Å.

The $[Ni(mnt)_2]^-$ ions are tilted by about 40° to the stack axis, as shown in Fig. 5. In addition alternate anions are rotated by 90° in the plane of the anion, such that the local anion · · · anion juxtaposition has long axial Ni · · · S interactions of 3.53 and 3.58 Å. Weak hydrogen bonds between CH of the phenyl groups and the more negative S and N locations on the metal complex anion occur, with near linear CH · · · N separations as short as 2.57 Å, and typically 2.70–2.75 Å, and the shortest CH · · · S contact is 3.16 Å.

The P · · · P separation in the LIT4PE tertiary motif in **5** at 8.2 Å is outside the normal range of 6.7 to 7.8 Å. This implies only slight weakening, because the energy dependence on P · · · P is relatively flat. The reason for the elongation is probably the local interaction between $[Ni(mnt)_2]^-$ anions shown in Fig. 5, which determines the repeat length of the anion and cation columns. There are two monoanions per repeat in the anion stack, and one cation per repeat in the cation column, but twice as many cation columns as anion stacks.

The structure of the salt $[MePh_3P][Ni(mnt)_2]$ (CSD refcode PMPESN) was determined by Fritchie in 1966.[27] The crystal packing of the salt was analysed and presciently described as offset stacks of anions separated by chains of interacting $[MePh_3P]^+$ cations. Here we develop this analysis, to compare and contrast with the structures of **4** and **5**. A projection along

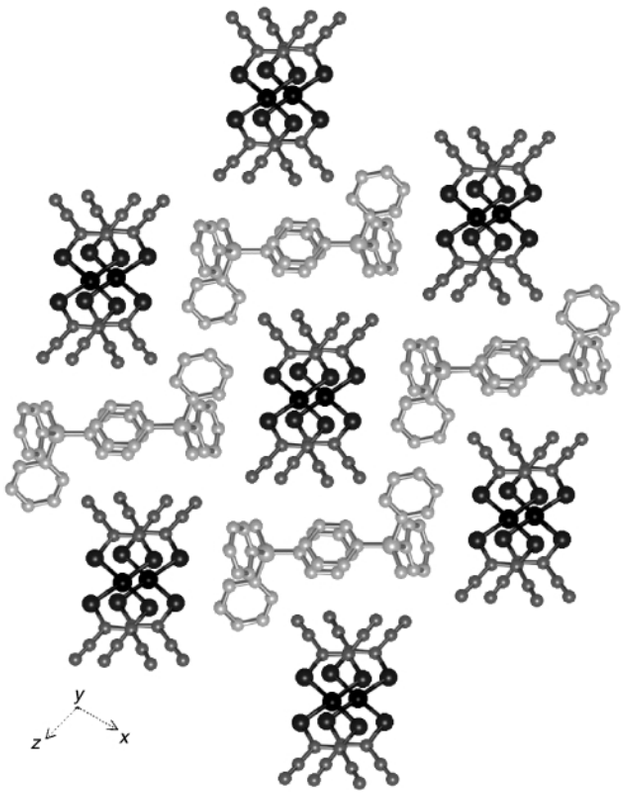

Fig. 6 Projection of the crystal structure of $[MePh_3P][Ni(mnt)_2]$ (PMPESN) along the stacking axis, showing the stacks of anions (dark tones) and the chains of cations (light tones). Hydrogen atoms are omitted.

the stacking axis is shown in Fig. 6. The anions form stacks of face-to-face pairs with a plane–plane separation of 3.54 Å within the pair and 3.71 Å between pairs. The $[MePh_3P]^+$ cation is unable to form the LIT4PE column, and instead forms a columnar tertiary motif containing prominent OFF interactions. The phenyl rings in these OFF interactions are parallel to the $[Ni(mnt)_2]^-$ planes, and equivalently spaced (see Supplementary Fig. S4). As in the other structures, there are hydrogen bonds from the cations to the anions (see Supplementary Fig. S5).

The $[MePh_3P]^+ \cdots [MePh_3P]^+$ motifs in PMPESN are novel. Pairs of cations form good parallel 4PEs, a secondary motif comprised of the OFF interaction already identified, and two vertex-to-face (VF) interactions. These P4PEs are then stacked so that the OFF interactions are parallel, to generate the column. This allows additional EF interactions between phenyl rings in adjacent P4PE motifs. These features are shown in Fig. 7. The full tertiary motif for the $[MePh_3P]^+$ cations in these crystals contains OFF, VF, and EF primary motifs, and P4PE secondary motifs.

The anion stacking described here between singly charged, planar $[M(mnt)_2]^-$ (M = Ni or Cu) molecules is similar to that observed in the crystal structures of other $[M(mnt)_2]^-$ salts containing non-planar counter ions, such as $[NR_4]^+$ (R = H, Me, Et or Bu).[18,38,39] The anion packing varies slightly between structures, forming stacks of dimers as in the case of $[MePh_3P][Ni(mnt)_2]$, or evenly spaced chains, as in the structure of **5**. In **5** and in PMPESN the columnar supramolecular motifs adopted by the phenylated cations have reinforced the anion stacking motifs. A question raised for such compounds is the balance of supramolecular energies contributed by the cation columns, the anion stacks, and the hydrogen bonds between them.

Dimeric dianions: $[\{M(mnt)_2\}_2]^{2-}$. Crystalline $[Ph_4P]_2[\{Co(mnt)_2\}_2]$ **6** and $[Ph_4P]_2[\{Fe(mnt)_2\}_2]$ **7** are isomorphous, and contain parallel stacks of anions and columns of cations in

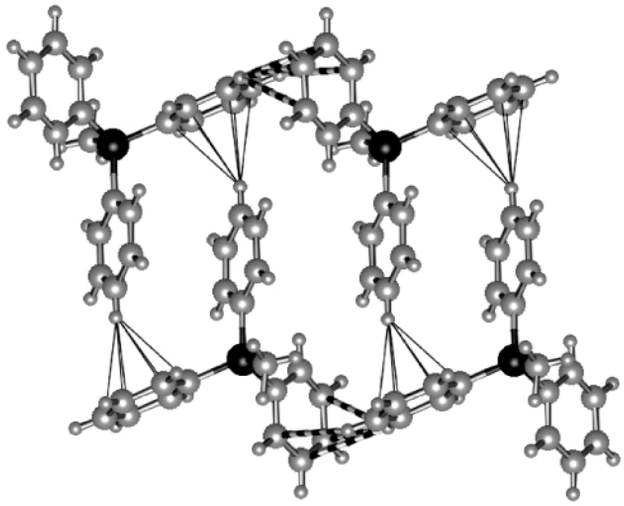

Fig. 7 Part of the column of $[MePh_3P]^+$ cations in PMPESN. The stack of OFF motifs in the centre is formed by a stacking of P4PE secondary motifs comprising two VF (thin lines) and one OFF between a pair of cations. In addition there are EF motifs (candystripes) between contiguous P4PEs. The methyl groups are not involved.

the LIT4PE motif. Fig. 8 is the projection along the columnar axis, and Fig. 9 shows how the stacking of the anions is commensurate with the translation of the cations in the LIT4PE column. The repeat distance (=*a*) is 7.14 Å. This lattice is similar to that of the monomeric monoanions, shown in Fig. 4: again there are six columns of cations surrounding a stack of anions. The main differences are (i) the anions in **6** are not alternately rotated by 90° as in **5**, (ii) the 'dish' distortion of the $\{Co(mnt)_2\}^-$ moieties prevents a planar overlap between neighbouring anions, (iii) the $[\{Co(mnt)_2\}_2]^{2-}$ anions are close to perpendicular to the stack axis, in contrast to the canted $[Ni(mnt)_2]^-$ ions in **5**, allowing a shorter repeat distance and a normal P · · · P separation in the T4PE of **6**. As in the preceding structures, there is a considerable number of C–H · · · N and some C–H · · · S hydrogen bonds (see Supplementary Fig. S6).

Octahedral dianions: $[M(mnt)_3]^{2-}$. Two crystal forms of $[Ph_4P]_2[Fe(mnt)_3]$ **8** have been structurally characterised so far. The dimorphs are readily identified by inspection of the crystals grown for diffraction studies. Those with a cubic habit have orthorhombic crystal symmetry (denoted α-**8**) whereas those that are diamondoid have monoclinic symmetry (denoted β-**8**). The structures of $[AsPh_4]_2[M(mnt)_3]$ (M = Fe, Mo, Tc or W) have previously been determined, and each is orthorhombic and isostructural with α-**8**.

The crystal lattice of α-**8** contains octahedral $[Fe(mnt)_3]^{2-}$ dianions surrounded by six $[Ph_4P]^+$ cations, without any anion · · · anion contacts. The cations form good P4PE. The principal feature of the crystal packing is a zig-zag chain of cations, with alternating P4PE and a twisted 6PE along the chain. The twisting of the 6PE is such that two phenyl rings are parallel and form a sandwich around one of the mnt ligands of the anion. The chain and the sandwich motifs are shown in Fig. 10. The chain is convex at the sandwich, and the concave side, between two P4PE, accommodates the other two mnt ligands of adjacent $[Fe(mnt)_3]^{2-}$ ions with C–H · · · N hydrogen bonds. There is also a well-developed C–H · · · S hydrogen bond (see Fig. 10). Fig. 11 shows detail of the two OFF motifs of the sandwich: the Ph · · · mnt plane separations are 3.5 Å.

The oxidised chromium complex salt, $[Ph_4P]_2[Cr(mnt)_3]$, **10**, forms black rhombohedral crystals isostructural with α-**8**.

The monoclinic form of $[Ph_4P]_2[Fe(mnt)_3]$, β-**8**, contains clearly defined layers of mixed ions parallel to the *ab* plane (see Supplementary Fig. S7). Each $[Fe(mnt)_3]^{2-}$ ion is surrounded by eight $[Ph_4P]^+$ cations, six of which are in the same layer as the anion, and two are in adjacent layers. Within the layers, the

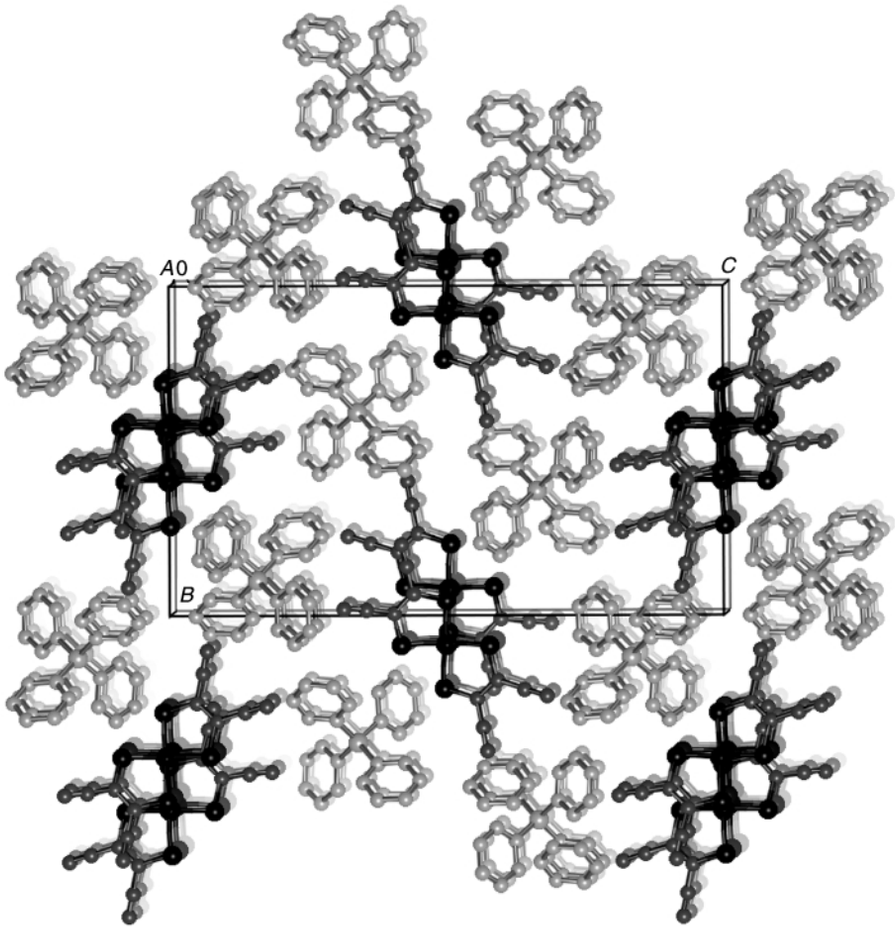

Fig. 8 The crystal packing of $[Ph_4P]_2[\{Co(mnt)_2\}_2]$ **6** viewed almost along the *a*-axis (space-group $P2_1/n$) to show the parallel stacks of $[\{Co(mnt)_2\}_2]^{2-}$ ions and columns of $[Ph_4P]^+$ cations.

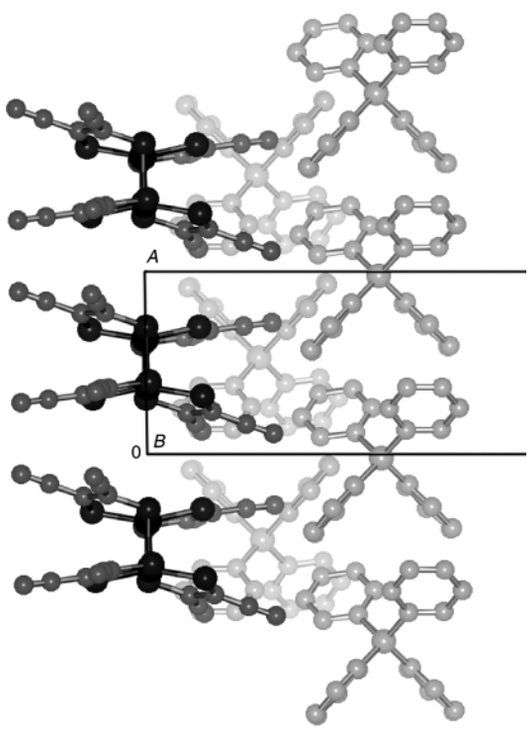

Fig. 9 The stack of $[\{Co(mnt)_2\}_2]^{2-}$ anions and two adjacent columns of $[Ph_4P]^+$ cations forming LIT4PE motifs, in **6**.

cations form zig-zag chains, with contiguous pairs of cations in the chain forming the sandwich motif with a mnt ligand (see Fig. 12). The sandwich secondary motif comprised of two Ph···mnt OFF primary motifs has no symmetry, and the planes are not exactly parallel. Each $[Fe(mnt)_3]^{2-}$ forms two sandwiches with $[Ph_4P]^+$ in different chains, each $[Ph_4P]^+$ forms two sandwiches, each pair of $[Ph_4P]^+$ forms one sandwich, and sandwich motifs occur on alternating sides of the chains. None of the standard secondary motifs formed by $[Ph_4P]^+$ is present. The zig-zag chain of $[Ph_4P]^+$ ions is similar to the commonly observed ZZI6PE, but the 6PE are instead intercalated by the mnt ligands forming sandwich motifs. The prevalence of the sandwich motif in this crystal structure, at the expense of more common motifs, signifies its favourabililty. As with α-**8**, the sandwiched mnt ligands form weak C–H···N hydrogen bonds to other phenyl rings of the $[Ph_4P]^+$. The unsandwiched mnt ligand is hydrogen bonded to phenyl groups from the cations in the adjacent layers: these phenyl rings are perpendicular to the mnt ligand, giving near linear C–H···S contacts of 2.97 Å (see Supplementary Fig. S8).

The significant features of the dimorphs of $[Ph_4P]_2[Fe(mnt)_3]$ **8** are the appearance of the sandwich Ph···mnt···Ph primary motif, and the occurrence of one sandwich and one P4PE in α-**8** and sandwiches only in β-**8**. This implies that the significance of the P4PE and the sandwich motifs are similar, but it must be recognised that there are different degrees of C–H···N and C–H···S hydrogen bonding in the two structures.

Octahedral trianion: $[Cr(mnt)_3]^{3-}$. The slow diffusion of a concentrated solution of $[Ph_4P]_3[Cr(mnt)_3]$ **9** in acetone into diethyl ether gave crystals solvated by 0.75 acetone molecules per formula unit. Crystals suitable for single crystal X-ray diffraction studies could not be cultivated from any other solvent system, indicating that the inclusion of acetone is necessary for the formation of a stable crystal lattice. Complex **9** is the first

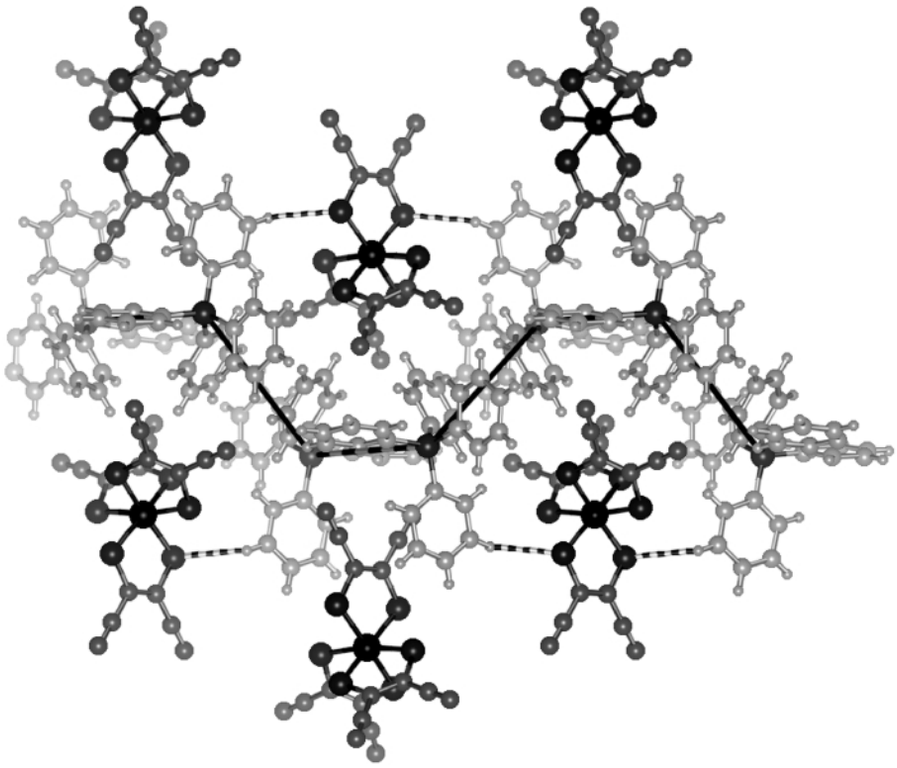

Fig. 10 The principal motif in the crystal packing of $[Ph_4P]_2[Fe(mnt)_3]$ α-**8**. The chain of $[Ph_4P]^+$ ions comprises alternating P4PE (black P—P connections, P · · · P 8.40 Å) and twisted 6PE (candystripe P—P connections) which form sandwiches around one mnt ligand of $[Fe(mnt)_3]^{2-}$. There are twofold axes, vertical in this picture, through Fe and the sandwich motif. The good C–H · · · S hydrogen bond (H · · · S 2.78 Å) is marked as a candystripe.

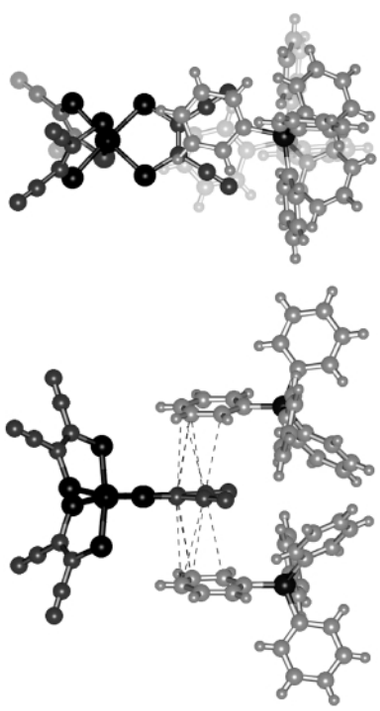

Fig. 11 Views normal and parallel to the $[Ph_4P]^+ \cdots [Fe(mnt)_3]^{2-} \cdots [Ph_4P]^+$ sandwich motif in $[Ph_4P]_2[Fe(mnt)_3]$ α-**8**. The motif has crystallographic twofold symmetry.

trianionic tris(dithiolene) complex to be characterised crystallographically, and it allows investigation of the crystal packing effect of three $[Ph_4P]^+$ cations per anion in the lattice. The incorporation of the solvent molecules suggests an inability to form good motifs with this stoichiometry. Moreover, the absence of previous crystal structures of trianionic tris(dithiolene) complexes implies that crystallisation of such salts occurs only under limited conditions.

As shown in Fig. 13, the structure of **9**·0.75Me_2CO comprises a complex labyrinth of cations formed around well separated anions. There are no intermolecular P · · · P separations indicative of good multiple phenyl embraces, but rather several interactions with P · · · P distances between 7.2 and 7.9 Å. Each of these interactions has the geometry of an offset 6PE in which six phenyl rings from the two neighbouring cations are engaged in six EF interactions. However, the offset nature of the interaction and the distances between phenyl rings imply that these interactions between cations are relatively weak. The manner in which the cations surround the anions permits the formation of many weak hydrogen bonds between the cations and the large, negatively charged surface of the anions: the CH · · · N and CH · · · S separations are typically *ca.* 2.70 and 2.90 Å respectively. The acetone solvent molecules fit into crevices in the cation networks, with several weak C–H · · · O hydrogen bonds to the carbonyl oxygen molecules, the shortest contact being 2.81 Å.

Molecular volumes and crystal packing coefficients

Computation of the Connolly surfaces of the constituent ions and solvent molecules in the crystal structures of **1**–**10** gives an indication of the relative size of the ions and permits the calculation of the packing coefficient, *k*,[40] for each structure. The packing coefficient, *k*, is defined as the ratio of the total molecular volume to the volume available in the condensed phase: crystals of organometallic compounds typically have *k* values of 0.60–0.70.

The values of *k* computed for the structures of **1**–**10** are between 0.65 and 0.69 (Supplementary Table T2). We note that the highest values for *k* are calculated for **2**, **3**, and **6**, each of which have close multiple phenyl embraces between cations; the structures with marginally lower *k* values have disrupted or no close cation · · · cation interactions.

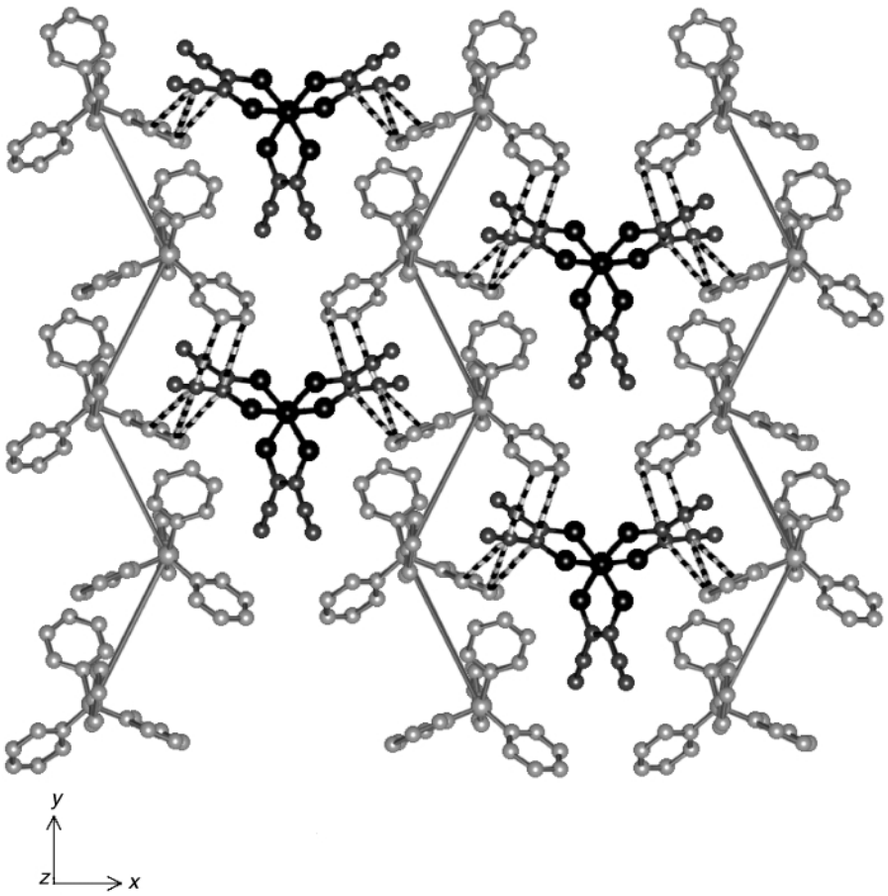

Fig. 12 The layer in $[Ph_4P]_2[Fe(mnt)_3]$, β-**8**. The zig-zag chains of $[Ph_4P]^+$ ions are marked with thin lines, and the sandwich motifs are indicated by candystripes for C(cation)···C(anion) distances <3.6 Å. Each $[Fe(mnt)_3]^{2-}$ forms two sandwiches with $[Ph_4P]^+$ in different chains.

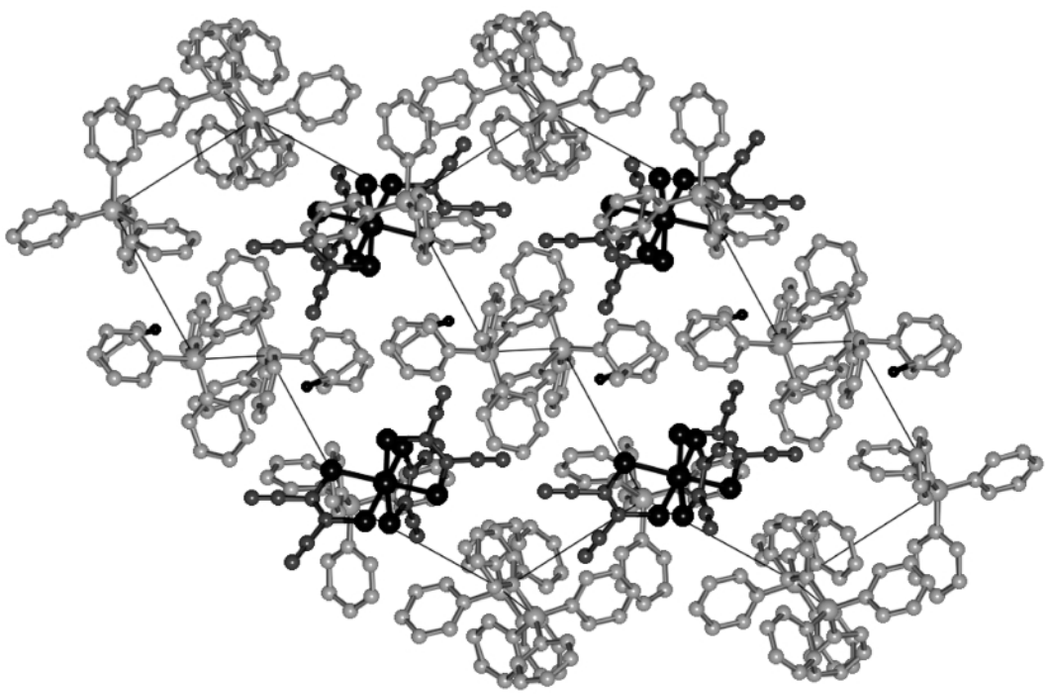

Fig. 13 The array of $[Ph_4P]^+$ (light), $[Cr(mnt)_3]^{3-}$ (dark) and acetone (○ black) in $[Ph_4P]_3[Cr(mnt)_3]\cdot 0.75Me_2CO$, **9**·$0.75Me_2CO$. The thin connections indicate the poorly developed offset 6PE motifs between cations.

Intermolecular energies

A new supramolecular motif has been recognised in the structures of **1**, α-**8** and β-**8**, namely OFF interactions between phenyl rings and mnt ligands. The structure of **1** contains individual OFF Ph···mnt contacts, for which the total interaction energy {for $[Ph_4P]^+$ plus $[Zn(mnt)_2]^{2-}$} is calculated to be −20.8 kcal mol^{-1} (van der Waals component −6.4 kcal mol^{-1}, electrostatic component −14.4 kcal mol^{-1}). The two dimorphs, α-**8** and β-**8** contain Ph···mnt···Ph sandwich motifs. The total interaction energy for this motif in β-**8** is calculated to be −32.1 kcal mol^{-1} {per $2[Ph_4P]^+$ plus $[Fe(mnt)_3]^{2-}$; van der Waals

component −15.2 kcal mol^{-1}, electrostatic component −16.9 kcal mol^{-1}}, marginally more attractive than the analogous interaction in α-**8**, computed as −30.6 kcal mol^{-1} (van der Waals −13.9 kcal mol^{-1}, electrostatic −16.7 kcal mol^{-1}). These cation···anion sandwich motifs are more attractive than multiple phenyl embraces.‡

Discussion and conclusions

Seven different crystal packings have been described for salts $[Ph_4P]_m[M(mnt)_n]$. Amongst these there is one general class of crystal packing clearly evident, which is the occurrence of chains (linear or almost linear) of embracing $[Ph_4P]^+$ cations between parallel chains or stacks of anions. This columnar packing type occurs with planar $[M(mnt)_2]^{2-}$ (**2** and **3**), planar $[M(mnt)_2]^-$ (**4** and **5**), and concave dimers $[\{M(mnt)_2\}2]^{2-}$ (**6** and **7**). Where the general shape of the anion does not allow this, as in non-planar tetrahedral (**1**) and octahedral anions (both forms of **8**, and **9** and **10**), the crystal packing is dominated by interactions between ions of opposite charge. Thus a first conclusion is that anion stacking, where possible, operates in concert with established columns of cations.

The charge difference between planar $[M(mnt)_2]^{2-}$ and planar $[M(mnt)_2]^-$ is a lesser factor, allowing the LIT4PE tertiary motif for $[Ph_4P]^+$ with $[M(mnt)_2]^-$, and a modification, the less common –6PE–OFF– chain, for $[Ph_4P]^+$ with $[M(mnt)_2]^{2-}$. The LIT4PE occurs in **4** and **5** with $[M(mnt)_2]^-$, and in **6** and **7** with $[\{M(mnt)_2\}_2]^{2-}$, with rather similar crystal packing which reflects the comparable shape and charge density for these two groups of anions. It is significant that the ZZI6PE motif which is common in other crystals containing $[Ph_4P]^+$ does not occur at all with these anions. It is possible to postulate and model a crystal lattice containing a ZZI6PE chain of $[Ph_4P]^+$ with a commensurate column of moderately canted $[M(mnt)_2]^{2-}$ anions. What is observed instead in **2** and **3** is a larger canting of the anions in order that the stack be linearly commensurate with the –6PE–OFF– chain, which is longer than the ZZI6PE chain. What is the reason for this subtle difference? We believe that it is found in the subtleties of local orientation and juxtaposition along the linear sequences of cations and anions, and attributed to the effects of CH···N and CH···S weak hydrogen bonding between cations and anions in adjacent columns. These CH···N and CH···S interactions are present in all structures.

It is significant that all crystals except $[Ph_4P]_3[Cr(mnt)_3]$, **9** are devoid of solvent. Since the inclusion of non-hydrogen-bonding solvent in lattices is often an indicator of shape awkwardness, we conclude that there is generally effective crystal packing, and that the spikeyness of the anions has been accommodated.

An important issue is the possibility of embrace motifs between $[Ph_4P]^+$ cations and the complex anions, because both have planar sections on their molecular surfaces: the occurrence of favourable EF and OFF motifs between oppositely charged ions can be considered. There is no evidence of such EF motifs, and therefore there are no hetero embraces analogous to multiple phenyl embraces. However, the planar segments of cations and anions participate in OFF motifs, as Ph···mnt···Ph sandwiches, that appear in the structures of $[Ph_4P]_2[M(mnt)_3]$. The dimorphs of $[Ph_4P]_2[M(mnt)_3]$, with one and two sandwich motifs per anion, suggest that this sandwich motif is favourable, and the calculated inter-ion energies support this conclusion. Why then is the sandwich motif not more frequently observed in these crystal structures? We suggest, on the basis of just these two structures, that this is because the sandwich motif interferes with other multiple phenyl embraces between the $[Ph_4P]^+$ cations. The dimorph α-**8** possesses one P4PE and one sandwich, and β-**8** has no multiple phenyl embraces with the two sandwiches.

We note also that the sandwich motif seems unsuited for the crystal packing of planar $[M(mnt)_2]^\varepsilon$ ions, because the phenyl rings on the same side of adjacent mnt rings would then be edge-to-edge. While this is not unknown,[41] it is not favourable, and separated chains of cations and anions are more favourable than interleaved anions and cations in sandwich motif.

The cation $[MePh_3P]^+$ is best suited to the formation of 6PEs and HA6PE lattices with threefold symmetry in crystals with other anions,[4,5,42] and as such does not support columnar lattice packing with segregated cations and anions. However, in the one compound with a $[Ni(mnt)_2]^-$ anion, it is able to support the anion stacking by stacking P4PE motifs and reinforcing these with additional EF interactions. It will be interesting to observe whether this new inter-cation motif occurs in other crystals with anion stacks or anion columns. In $[MePh_3P]_2[Cu_3Br_8]$ there are segregated chains of anions and cations, which use pseudo-6PE involving methyl to propagate a ZZI6PE tertiary motif.[9]

We conclude with our understanding of the crystal supramolecularity of the structures reported here. Where there are anions which are planar (**2**, **3**, **4**, **5**) or approximately planar (**6**, **7**) the linear column of 4PE (**4**, **5**, **6**, **7**) or the approximately linear column of –6PE–OFF– (**2**, **3**) matches well with an anion stack which is linear or approximately linear. Details of the commensurability of the repetition in these linear parallel motifs are determined not by the favourable repeat in the separated cation and anion chains, but by the prevalent but weak hydrogen bonds from cation to anion. Where the anions are not fully planar (but tetrahedral or octahedral), OFF interactions between planar mnt subsections of the anions and planar phenyl subsections of the cations occur, as a concerted motif with four ions (**1**) or as the sandwich motif (α-**8**, β-**8**). In these cases the cation to anion hydrogen bonds continue to be significant. The one remaining crystal (**9**) with an octahedral anion and three cations per anion forms poorer cation motifs despite the high proportion of cations in the crystal volume: it relies on hydrogen bonding, and fills space in awkward packing with solvent acetone.

Experimental

Synthesis

The complexes $[Ph_4P]_2[Zn(mnt)_2]$, $[Ph_4P]_2[Cu(mnt)_2]$, $[Ph_4P][Cu(mnt)_2]$, $[Ph_4P]_2[Ni(mnt)_2]$, $[Ph_4P][Ni(mnt)_2]$, $[Ph_4P]_2[\{Co(mnt)_2\}_2]$, $[Ph_4P]_2[\{Fe(mnt)_2\}_2]$, $[Ph_4P]_2[Fe(mnt)_3]$, $[Ph_4P]_3[Cr(mnt)_3]$, and $[Ph_4P]_2[Cr(mnt)_3]$ were prepared by adaptation of methods published for other cations.[43–47] The salts are air-stable in the solid-state and are soluble in common polar organic solvents, such as acetone, CH_2Cl_2, MeCN, $MeNO_2$ and DMSO. Microanalyses were carried out by the Campbell Microanalytical Laboratory, University of Otago, Dunedin, New Zealand.

$[Ph_4P]_2[Cr(mnt)_3]$. To a brown solution of $[Ph_4P]_3[Cr(mnt)_3]$ (100 mg, 0.07 mmol) in CH_2Cl_2 (10 cm^3) was added a solution of iodine (8 mg, 0.04 mmol) in CH_2Cl_2 (5 cm^3) to give an immediate black solution. After stirring for 15 min, gradual addition of *n*-hexane induced the formation of a fine microcrystalline precipitate, which was collected, washed with diethyl ether and dried under vacuum. Yield 61 mg, 76%.

Crystallography

All diffraction measurements were made at 298 K, with the

‡ For comparison, the net attractive energies for 6PEs between $[Ph_4P]^+$ cations are typically in the range 7–10 kcal mol^{-1} (van der Waals typically 9–14 kcal mol^{-1} attraction, net coulombic repulsion typically 4–6 kcal mol^{-1}). In general, the two types of 4PEs are slightly less attractive, both O4PEs and P4PEs between $[Ph_4P]^+$ cations typically in the range 5–9 kcal mol^{-1}.

crystals mounted on a glass fibre using epoxy glue. Crystal data and refinement details are given in Table 2. Lorentz, polarisation and absorption corrections were applied. The structures were solved and refined using the SHELXTL crystallographic software package.[48] All non-hydrogen atoms were assigned anisotropic displacement parameters. Hydrogen atoms were constrained to idealised positions. The occupancy of the acetone solvent molecule in the structure of **9** was assigned as 0.75 after refinement.

CCDC reference number 186/2105.

See http://www.rsc.org/suppdata/dt/b0/b000093k/ for crystallographic files in .cif format.

Acknowledgements

We thank D. C. Craig for collection of the X-ray diffraction data for compounds **2**, **3**, **5** α-**8** and β-**8**. G. R. L. wishes to thank the Royal Society for a Fellowship Tenable Overseas. This research is supported by the Australian Research Council.

References

1 I. G. Dance and M. L. Scudder, *J. Chem. Soc.*, *Chem. Commun.*, 1995, 1039.
2 I. Dance and M. Scudder, *Chem. Eur. J.*, 1996, **2**, 481.
3 I. Dance and M. Scudder, *J. Chem. Soc.*, *Dalton Trans.*, 1996, 3755.
4 C. Hasselgren, P. A. W. Dean, M. L. Scudder, D. C. Craig and I. G. Dance, *J. Chem. Soc.*, *Dalton Trans.*, 1997, 2019.
5 M. Scudder and I. Dance, *J. Chem. Soc.*, *Dalton Trans.*, 1998, 329.
6 M. Scudder and I. Dance, *J. Chem. Soc.*, *Dalton Trans.*, 1998, 3155.
7 M. Scudder and I. Dance, *J. Chem. Soc.*, *Dalton Trans.*, 1998, 3167.
8 G. R. Desiraju and T. Steiner, *The weak hydrogen bond in structural chemistry and biology*, Oxford University Press, Oxford, 1999.
9 S. Lorenzo, C. Horn, D. Craig, M. L. Scudder and I. G. Dance, *Inorg. Chem.*, 2000, **39**, 401.
10 J. A. McCleverty, *Prog. Inorg. Chem.*, 1968, **10**, 49.
11 R. Eisenberg, *Prog. Inorg. Chem.*, 1970, **12**, 295.
12 D. Coucouvanis, *Prog. Inorg. Chem.*, 1970, **11**, 233.
13 R. P. Burns and C. A. McAuliffe, *Adv. Inorg. Chem. Radiochem.*, 1979, **22**, 303.
14 S. Alvarez, R. Vicente and R. Hoffmann, *J. Am. Chem. Soc.*, 1985, **107**, 6253.
15 R. T. Henriques, L. Alcacer, D. Jerome, C. Bourbonnais and C. Weyl, *J. Phys. C.*, 1986, **19**, 4663.
16 L. Alcacer, *Mol. Cryst. Liq. Cryst.*, 1985, **120**, 221.
17 R. T. Henriques, L. Alcacer, M. Almeida and S. Tomic, *Mol. Cryst. Liq. Cryst.*, 1985, **120**, 237.
18 A. T. Coomber, D. Beljonne, R. H. Friend, J. L. Bredas, A. Charlton, N. Robertson, A. E. Underhill, M. Kurmoo and P. Day, *Nature* (*London*), 1996, **380**, 144.
19 H. Kisch, *Comments Inorg. Chem.*, 1994, **16**, 113.
20 H. Kisch, *Coord. Chem. Rev.*, 1997, **159**, 385.
21 L. Golic, W. Dietzsch and R. Kirmse, *Vestn. Slov. Kem. Drus.*, 1987, **34**, 401.
22 J. Stach, R. Kirmse, J. Sieler, U. Abram, W. Dietzsch, B. Bottcher, L. K. Hansen, H. Vergoossen, M. C. M. Gribnau and C. P. Keijzers, *Inorg. Chem.*, 1986, **25**, 1369.
23 L. Golic, W. Dietzsch, K. Kohler, J. Stach and R. Kirmse, *J. Chem. Soc.*, *Dalton Trans.*, 1988, 97.
24 A. Sequeira and I. Bernal, *J. Cryst. Mol. Struct.*, 1973, **3**, 157.
25 G. F. Brown and E. I. Stiefel, *Inorg. Chem.*, 1973, **12**, 2140.
26 S. F. Colmanet and M. F. Mackay, *Aust. J. Chem.*, 1988, **41**, 1127.
27 C. J. Fritchie, *Acta Crystallogr.*, 1966, **20**, 107.
28 A. J. Pertsin and A. I. Kitaigorodsky, *The atom–atom potential method. Applications to organic molecular solids*, Springer Series in Chemical Physics, Springer-Verlag, Berlin, 1987.
29 A. Gavezzotti, *Theoretical Aspects and Computer Modelling of the Molecular Solid State*, Molecular Solid State Series, John Wiley, Chichester, 1997.
30 I. G. Dance, in *The Crystal as a Supramolecular Entity*, ed. G. R. Desiraju, John Wiley, New York, 1996, pp. 137–233
31 G. R. Lewis and I. G. Dance, *J. Chem. Soc.*, *Dalton Trans.*, 2000, 299.
32 A. K. Rappe and W. A. Goddard, *J. Phys. Chem.*, 1991, **95**, 3358.
33 CERIUS^2 molecular modelling software, MSI/Biosym Inc., San Diego, 1998, http://www.msi.com.
34 M. L. Connolly, *Science*, 1983, **221**, 709.
35 M. L. Connolly, *J. Am. Chem. Soc.*, 1985, **107**, 1118.
36 V. M. Russell, *Crystal Supramolecular Chemistry of Metal Complexes containing Phenanthroline and Oxalate Ligands, and Associated Phenylated Cations*, BSc Honours thesis, University of New South Wales, Sydney, 1999.
37 V. M. Russell, I. G. Dance and M. L. Scudder, *J. Chem. Soc.*, *Dalton Trans.*, submitted.
38 B. L. Ramakrishna, *Inorg. Chim. Acta*, 1986, **114**, 31.
39 P. I. Clemenson, A. E. Underhill, M. B. Hursthouse and R. L. Short, *J. Chem. Soc.*, *Dalton Trans.*, 1988, 1689.
40 A. I. Kitaigorodskii, *Molecular Crystals and Molecules*, Academic Press, New York, 1973.
41 M. L. Scudder and I. G. Dance, *CrystEngComm.*, 1999, **8**, 1.
42 C. Horn, I. G. Dance, D. Craig, M. L. Scudder and G. A. Bowmaker, *J. Am. Chem. Soc.*, 1998, **120**, 10549.
43 A. Davidson and R. H. Holm, *Inorg. Synth.*, 1972, **15**, 9.
44 A. Davidson, N. Edelstein, R. H. Holm and A. H. Maki, *Inorg. Chem.*, 1963, **2**, 1227.
45 J. F. Weiher, L. R. Melby and R. E. Benson, *J. Am. Chem. Soc.*, 1964, **86**, 4329.
46 M. Gerloch, S. F. A. Kettle, J. Locke and J. A. McCleverty, *Chem. Commun.*, 1966, 29.
47 A. Davidson, N. Edelstein, R. H. Holm and A. H. Maki, *J. Am. Chem. Soc.*, 1964, **86**, 2799.
48 SHELXTL, Rev. 5.10, Bruker AXS, Madison, WI, USA.